

Ab initio study of the energetics and thermodynamics of hydrogen abstraction from fluoromethanes by O(³P). II: CF_nH_{4-n} + O(³P) → CF_nH_{4-n}...O → ·CF_nH_{3-n} + ·OH (n = 0, 1, 2)

W.C. Kreye^{a,*}, Paul G. Seybold^b

^a *CaTS/Research and Instruction Computer Center, Wright State University, Dayton, OH 45435, USA*

^b *Chemistry Department, Wright State University, Dayton, OH 45435, USA*

Received 27 September 2000; in final form 22 November 2000

Abstract

Hydrogen abstractions by O(³P) from a set of fluorinated methanes, CF_nH_{4-n} + O(³P) → CF_nH_{4-n}...O → ·CF_nH_{3-n} + ·OH (n = 0, 1, 2), were studied using ab initio methods. Geometries of the reactants and transition states were optimized at the UMP2/6-311G** level of theory, and activation energies were calculated using a modified GAUSSIAN 2 (\hat{G}_2) theory. The potential-energy curves for the transition states were computed in order to obtain the transmission coefficients, κ , for the reactions studied. We found that $\kappa_{\text{aver}} = 1.12 \pm 0.01$. Activation energies, activation enthalpies and rate constants were computed. Good agreement, (the average difference is 0.9 ± 0.4 kcal/mol for the present study), was found between the ab initio activation energies, $\Delta G_{\text{theor.}}^\ddagger$, and the experimental activation energies, $\Delta G_{\text{expt'l}}^\ddagger$. © 2001 Published by Elsevier Science B.V.

1. Introduction

The reactions of halogenated hydrocarbons with oxygen are important in atmospheric chemistry [1], where such reactions have been implicated in damage to the ozone layer; in environmental studies, since members of this class have entered the land and water as pollutants; and in biochemistry, where oxidative metabolism of these compounds can sometimes lead to toxic products [2–4].

An especially important reaction for halogenated hydrocarbons is hydrogen abstraction by O(³P). In a recent Letter, Kreye [5] presented a theoretical study of hydrogen abstraction from trifluoromethane by O(³P):



In that Letter he used a slightly modified G_2 , \hat{G}_2 , theory, and obtained a theoretical (ab initio) activation energy, $\Delta G_{\text{theor.}}^\ddagger = 15.0$ kcal/mol, which can be compared to the experimental activation energy, $\Delta G_{\text{expt'l}}^\ddagger = 17.3$ kcal/mol. He obtained excellent agreement between experimental and theoretical structures. Thus he established that G_2 theory is successful in dealing with transition-state (TS) energies, as well as with atomization and

* Corresponding author. Fax: +1-513-8733213.

E-mail address: wkreye@desire.cc.wright.edu (W.C. Kreye).

ionization energies. In order to further understand the effects of substituted F-atoms on the structures, thermodynamic properties, and reactions of the fluoromethanes, we have now examined the remaining members of the fluoromethane series: CF_2H_2 , CFH_3 and CH_4 . Activation energies, activation enthalpies, reaction enthalpies and rate constants have been determined, as well as structural parameters.

Early studies of hydrogen abstractions from methane and its halogenated derivatives have been reported [6,7]. Recently, Roberto-Neto et al. [8], have performed extensive studies of the reaction of CH_4 and $\text{O}(\text{}^3\text{P})$, including forward and reverse reactions. González et al. [9] have made an excellent and thorough study of the reaction between $\text{O}(\text{}^3\text{P})$ and CH_4 using ab initio methods. In a related study, Yamada et al. [10] have studied the kinetics and thermochemistry of the reaction of the OH radical with several Cl- and F-substituted ethanes. In the hydrogen abstraction from CH_4 by $\text{O}(\text{}^3\text{P})$, Gonzalez et al. [11] used POL-CI theory to obtain good agreement between experimental and calculated barrier heights.

2. Computational methods

In this study, the GAUSSIAN 98 [12] suite of programs was used with a slightly modified $G2$ theory for the energies. We designate this latter method by $\hat{G}2$. The modification consisted in using a higher-level optimized geometry, namely, UMP2/6-311G**, than is used in the conventional $G2$ theory [13]. Structures were optimized at the UMP2/6-311G** level, and UMP2 electronic energies, E , in the ground-vibrational state were computed. Zero-point energies (ZPE) and thermal (vibrational, rotational, and translational) energies and entropies at 298.15 K were included in the computations of ΔH , ΔG , ΔS . A vibrational scaling factor of 0.94 was used for the ZPE and thermal energies. Single-point energies were computed for all higher levels in the $\hat{G}2$ computations. Several of the higher levels used were UMP4/6-311G (2df, p), QCISD(T)/6-311G** and UMP2/6-311+G (3df, 2p). (See [13] for definitions of all the higher-levels.) The usual high-level corrections (HLC) [13]

were employed. The FREQ program was used at the UMP2/6-311** level to obtain the normal-mode frequencies, ZPE, thermal energy corrections to 298.15 K and entropy values. Hindered internal rotation corrections to E and S were not performed. With regard to the symmetry of the TS, Kreye [5] showed for the reactant, CF_3H , that the two symmetry states, ${}^3A'$ and ${}^3A''$, yielded the same structures and energies within computational uncertainty. Therefore, we performed computations for only a single symmetry state for each reactant. Also, it was assumed that concentrations of the ${}^3A'$ and ${}^3A''$ states were equal.

For the reaction path, the internal-reaction-coordinate (IRC) curve, developed by Gonzalez and Schlegel [14], was computed at the UMP2/6-311G** level. This IRC method yields a dependence of the energy E (UMP2/6-311G**) upon the internal-reaction-coordinate, s , with origin at the TS energy. The resulting potential-energy curve, $V(s)$ vs s , defines the minimum-energy path (MEP) for the reaction.

3. Theory

3.1. Rate constant

The absolute rate constant, k_{abs} , derived originally by Glasston et al. [15] is based on classical statistical mechanics and the TS concept. In order to introduce quantum-mechanical tunneling through the potential barrier, a multiplicative transmission coefficient κ is employed, such that the final rate constant, $k = \kappa k_{\text{abs}}$. Thus, k can then be expressed in terms of thermodynamic quantities as

$$k = \kappa (k_{\text{B}}T/h) \exp(-\Delta H^\ddagger/RT) \exp(\Delta S^\ddagger/R). \quad (1)$$

(See [16] for a complete discussion of TS theory.) The above expression corresponds to the 'conventional' TS theory. Refinements such as the use of the microcanonical rate constant, the introduction of the microcanonical variation TS theory and the consideration of 'corner cutting' tunneling corrections through the 'walls' of the potential surface, as described in [16], are not employed in the present study.

Also, at $T = 298.15$ K, we define

$$k_{\text{theor.}} (\text{cm}^3/\text{mol s}) \\ = \kappa 1.5199 \times 10^{17} \exp(-\Delta G_{\text{theor.}}^\ddagger/RT). \quad (2)$$

3.2. Transmission coefficient

The present study uses the semi-classical approximation transmission coefficient defined in [17] as:

$$\kappa = 1 + (2/k_{\text{B}}T) \int_{E_0}^{V_{\text{max}}} P(E) \sinh[(V_{\text{max}} - E)/k_{\text{B}}T] dE, \quad (3)$$

where $P(E)$ is the semi-classical approximation to the transmission probability. It is defined in terms of the potential energy curve, $V(s)$ vs s , which is obtained from the IRC method. In the region, $E_0 \leq E \leq V_{\text{max}}$, $P(E)$ is defined as

$$P(E) = \left(1 + \exp \left\{ 2\hbar^{-1} \int_{s \leq}^{s \geq} (2\mu)^{1/2} \right. \right. \\ \left. \left. \times [(V(s) - E)^{1/2}] ds \right\} \right)^{-1}, \quad E_0 \leq E \leq V_{\text{max}}. \quad (4)$$

V_{max} is the maximum in the $V(s)$ vs s curve, μ is the reduced mass, $s \leq$ and $s \geq$ are the intersections of the E_0 line with that curve. E_0 is chosen in order that κ converges as E_0 is algebraically decreased. (In the earlier work by Kreye [5], utilization of the Kemble parabolic-potential model is described, and the values for κ are found to be in general agreement with the values obtained by the present method.)

3.3. Experimental activation energy $\Delta G_{\text{expt'l}}^\ddagger$

From the standpoint of the kinetics of the reaction, the activation energy is probably the most important thermodynamical quantity. We base the following derivation on [15]. In order to obtain an experimental activation energy, $\Delta G_{\text{expt'l}}^\ddagger$ to be compared with the theoretical activation energy, $\Delta G_{\text{theor.}}^\ddagger$ we must use the so-called experimental energy of activation, E_a , from the Arrhenius equation:

$$k_{\text{expt'l}} (\text{cm}^3/\text{mol s}) = [A T^n] \exp(-E_a/RT), \quad (5)$$

where A is a constant and where the standard state is unit concentration.

Now we can restate Eq. (1) in term of experimental quantities:

$$k_{\text{expt'l}} = \kappa (k_{\text{B}}T/h) \exp(-\Delta H_{\text{expt'l}}^\ddagger/RT) \exp(\Delta S_{\text{expt'l}}^\ddagger/R). \quad (6)$$

Ref. [15] shows that for a bimolecular reaction,

$$\Delta H_{\text{expt'l}}^\ddagger = E_a - 2RT. \quad (7)$$

Substitute Eq. (7) into Eq. (6) in order to eliminate $\Delta H_{\text{expt'l}}^\ddagger$. If the resulting expression for $k_{\text{expt'l}}$ is equated to Eq. (5), we obtain, after a rearrangement, an expression for $\Delta S_{\text{expt'l}}^\ddagger$ in terms of A :

$$\Delta S_{\text{expt'l}}^\ddagger = R \ln[A/(\kappa 3.767 \times 10^{15} T^{1-n})], \quad (8)$$

where we have substituted the numerical values of $e^2 k_{\text{B}}/h$ for the standard state of unit concentration.

Now substitute Eqs. (7) and (8) into

$$\Delta G_{\text{expt'l}}^\ddagger = \Delta H_{\text{expt'l}}^\ddagger - T \Delta S_{\text{expt'l}}^\ddagger. \quad (9)$$

We thus obtain an expression for $\Delta G_{\text{expt'l}}^\ddagger$ in terms of measured quantities (except for the calculated κ):

$$\Delta G_{\text{expt'l}}^\ddagger = (E_a - 2RT) \\ - RT \ln[A/(\kappa 3.767 \times 10^{15} T^{1-n})]. \quad (10)$$

4. Results

4.1. Structures

The theoretical and experimental [18] structures of the reactant, TS, and products are presented in Table 1 for the reactant, CF_2H_2 . The system was optimized at the UMP2/6-311G** level. The geometry and parameters of the $\text{CF}_2\text{H}_2 \dots \text{O}$ TS are displayed in Fig. 1. (The subscripts on the atoms in the bond-length and bond-angle designations should not be confused with the number of F and H atoms in the molecule designations.) The agreement between the theoretical and experimental bond distances is within ± 0.004 Å, and between the theoretical and experimental bond angles is within $\pm 1.2^\circ$. It can be seen that the

Table 1

Theoretical (ab-initio) and experimental [18] bond distances (Å) and bond angles (°) for $\text{CF}_2\text{H}_2 \dots \text{O}$ (symmetry $^3A'$), CF_2H_2 , and CF_2H^a

Geometric parameter	$\text{CF}_2\text{H}_2 \dots \text{O}$ theor.	CF_2H_2 theor.	CF_2H_2 expt'l.	CF_2H theor.
C–H ₂	1.264	1.090	1.092	1.087
H–O	1.206	–	–	–
C–H ₅	1.091	1.090	1.092	1.087
C–H ₆	1.334	1.356	1.358	1.327
C–H ₇	1.334	1.356	1.358	1.327
α_1 Angle O–H ₂ –C	88.83	–	–	–
α_2 Angle H ₅ –C–H ₂	107.95	113.13	111.9	–
α_3 Angle F ₆ –C–H ₂	107.57	108.66	–	–
α_4 Angle F ₇ –C–H ₂	107.57	108.66	–	–
α_5 Angle H ₅ –C–F ₇	111.49	108.68	–	113.64
α_6 Angle F ₆ –C–F ₇	110.55	108.95	108.3	111.51
Dihedral Angle ^b	120.44	120.79	–	–

^a Optimization level is UMP2/6-311G**. See Fig. 1 for definitions of the subscripts on the bond lengths and bond angles. Although Fig. 1 is for the TS, it can also be used for CF_2H_2 and CF_2H .

^b Dihedral angle is the angle between the F₆–C–H₂ plane and the XZ plane.

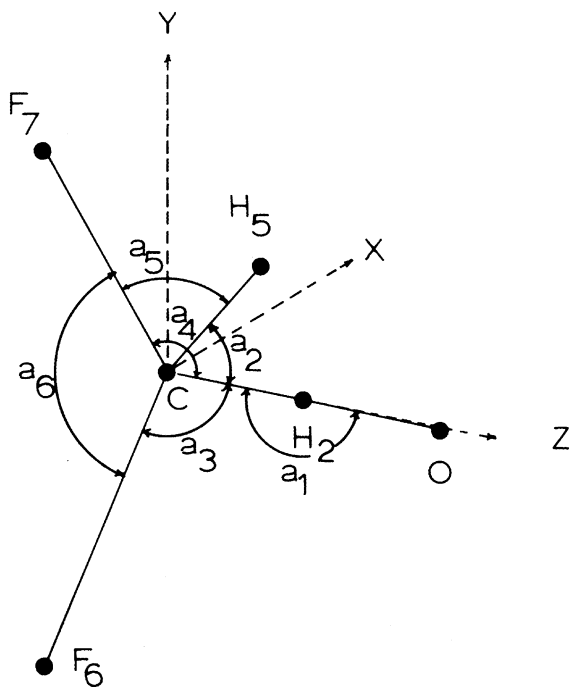


Fig. 1. Schematic representation of the structure of $\text{CF}_2\text{H}_2 \dots \text{O}$ TS, which has been optimized at the UMP2/6-311G** level. The C atom is at the origin, and the H₅, H₂, and O atoms are in the XZ plane. The F₇ and F₆ atoms are symmetrically located above and below the XZ plane. The values of the angles and distances are given in Table 1.

reacting-bond distance, C–H₂, in the parent compound is considerably increased when the O atom is added to form the TS. Similar results were found for the other two reactants, CFH_3 and CH_4 .

4.2. Activation enthalpies, entropies, and rate constants

The above thermodynamic quantities are given in Tables 2–4 for the reactants: CF_2H_2 , CFH_3 , and CH_4 , respectively. In general, the \hat{G}_1 values are a considerable improvement (towards the experimental values) over the UMP4/6-311G** energy values; but the \hat{G}_2 values only show a slight change from the \hat{G}_1 values. The average difference between the theoretical and experimental values of ΔG^\ddagger is 0.9 ± 0.4 kcal/mol for the present series in Tables 2–4. The difference between the experimental and theoretical values of ΔH_r for CH_4 in Table 4 is somewhat large, although there is no improvement in going from the UMP2/6-311G** level to the UMP4/6-311G** level.

4.3. Natural atomic charges

The natural atomic charges, Q_n , defined by Reed et al. [20], have been found by one of us (Paul G. Seybold) to be much better regression measures of molecular structural variations than

Table 2

Activation and reaction thermodynamic values from experimental data [19,18], respectively; and theoretical (ab-initio) computations at various levels at 298.15 K for the following reaction: $\text{CF}_2\text{H}_2 + \text{O}(^3\text{P}) \rightarrow \text{CF}_2\text{H}_2 \dots \text{O} \rightarrow \cdot\text{CF}_2\text{H} + \cdot\text{OH}$

Activation quantity	(UMP4/6-311G**)	\hat{G}_1	\hat{G}_2	Experimental
ΔH^\ddagger (kcal/mol)	+13.02 ^a	+7.51 ^a	+7.42 ^a	–
ΔS^\ddagger (cal/mol K)	–24.49	–24.49	–24.49	–
ΔG^\ddagger (kcal/mol)	+20.32	+14.81	+14.71	+15.34 ^b
k (cm ³ /mol s)	–	–	(27×10^5) ^c	(9×10^5) ^d
Reaction quantity	(UMP2/6-311G**)	–	–	–
ΔH_r (kcal/mol)	+1.79 ^a	–	–	–

^a System was optimized at the UMP2/6-311G** level, and there were included ZPE and thermal energy correction to 298.15 K with a scale factor of 0.94.

^b This term is $\Delta G_{\text{expt}^\ddagger}^\ddagger$, which is calculated from the data in [19] as described in Section 3.3. $\kappa = 1.104$.

^c See Eq. (2) for $k_{\text{theor.}}$.

^d Ref. [19]: Use $n = 0$, $A = 2.65 \times 10^{12}$ and $E_a = 8.802$ kcal/mol in Eq. (5).

Table 3

Activation and reaction thermodynamic values from experimental data, [19] and [18], respectively; and theoretical (ab-initio) computations at various levels at 298.15 K for the following reaction: $\text{CFH}_3 + \text{O}(^3\text{P}) \rightarrow \text{CFH}_3 \dots \text{O} \rightarrow \cdot\text{CFH}_2 + \cdot\text{OH}$

Activation quantity	(UMP4/6-311G**)	\hat{G}_1	\hat{G}_2	Experimental
ΔH^\ddagger (kcal/mol)	+12.25 ^a	+7.11 ^a	+6.97 ^a	–
ΔS^\ddagger (cal/mol–K)	–24.00	–24.00	–24.00	–
ΔG^\ddagger (kcal/mol)	+20.01	+14.27	+14.13	+15.62 ^b
k (cm ³ /mol s)	–	–	(75×10^5) ^c	(6×10^5) ^d
Reaction quantity	(UMP2/6-311G**)	–	–	–
ΔH_r (kcal/mol)	+0.88 ^a	–	–	–

^a System was optimized at the UMP2/6-311G** level, and there were included ZPE and thermal energy correction to 298.15 K with a scale factor of 0.94.

^b This term is $\Delta G_{\text{expt}^\ddagger}^\ddagger$, which is calculated from the data in [19] as described in Section 3.3. $\kappa = 1.132$.

^c See Eq. (2) for $k_{\text{theor.}}$.

^d Ref. [19]: Use $n = 0$, $A = 7.8 \times 10^{12}$ and $E_a = 9.696$ kcal/mol in Eq. (5).

Table 4

Activation and reaction thermodynamic values from experimental measurements, [19] and [18], respectively; and theoretical (ab-initio) computations at various levels at 298.15 K for the following reaction: $\text{CH}_4 + \text{O}(^3\text{P}) \rightarrow \text{CH}_4 \dots \text{O} \rightarrow \cdot\text{CH}_3 + \cdot\text{OH}$

Activation quantity	(UMP4/6-311G**)	\hat{G}_1	\hat{G}_2	Experimental
ΔH^\ddagger (kcal/mol)	+12.23 ^a	+7.25 ^a	+7.14 ^a	–
ΔS^\ddagger (cal/mol K)	–23.03	–23.03	–23.03	–
ΔG^\ddagger (kcal/mol)	+19.09	+14.10	+14.00	14.67 ^b
k (cm ³ /mol s)	–	–	(9.4×10^6) ^c	(3.0×10^6) ^d
Reaction quantity	(UMP2/6-311G**)	UMP4 ^e	–	–
ΔH_r (kcal/mol)	+4.45 ^a	+4.97	–	2.6

^a System was optimized at the UMP2/6-311G** level, and there were included ZPE and thermal energy correction to 298.15 K with a scale factor of 0.94.

^b This term is $\Delta G_{\text{expt}^\ddagger}^\ddagger$, which is calculated from the data in [19] as described in Section 3.3. $\kappa = 1.143$.

^c See Eq. (2) for $k_{\text{theor.}}$.

^d Ref. [19]: Use $n = 1.56$, $A = 6.9 \times 10^8$ and $E_a = 8.484$ kcal/mol in Eq. (5).

^e The full level is UMP4/6-311G**//UMP2/6-311G**.

Table 5

Experimental H–C bond dissociation enthalpies (BDE's) and theoretical atomic natural charges (Q_n)^a

Compound (Bond)	BDE _{expt'l}	ΔH_r^b	$Q_n(\text{C})^c$	$Q_n(\text{F})^c$	$Q_n(\text{H})^c$	$\Delta G_{\text{theor.}}^\ddagger$ ^d
CH ₃ –H	105.1 ^e	+4.45	–0.70 (–0.71)	–	+0.18 (+0.18)	+14.00
CFH ₂ –H	101.2 ^f	+0.88	+0.05 (+0.04)	–0.43 (–0.44)	+0.13 (+0.18)	+14.13
CF ₂ H–H	103.2 ^f	+1.79	+0.64 (+0.63)	–0.41 (–0.42)	+0.10 (+0.10)	+14.71
CF ₃ –H	106.2 ^{g,h}	+4.8	+1.11 (+1.11)	–0.40 (–0.40)	+0.08 (+0.09)	+15.0

^aTheoretical reaction enthalpies (ΔH_r) and theoretical activation energies ($\Delta G_{\text{theor.}}^\ddagger$) for hydrogen abstraction by O(³P). All energies have units of kcal/mol.

^bUMP2/6-311G** level, with ZPE and thermal energy correction to 298.15 K, including a 0.94 scaling factor for vibrations.

^cHF/6-311++G (2d, p) level, MP2//HF/6-311++G(2d,p) level values in parentheses.

^dSee Tables 2–4 and Ref. [5] for data.

^eRef. [22].

^fRef. [23].

^gRef. [24].

^hRef. [25].

the Mulliken and electrostatic atomic charges [21]. Table 5 lists the parent compounds, the values of Q_n for the three atoms, and the activation energies, $\Delta G_{\text{theor.}}^\ddagger$, for the hydrogen abstraction by (O³P). There is a reversal in carbon atomic charges and the fluorine charges remain approximately constant with fluorination. The hydrogen charges increase monotonically with decreasing number of fluorine atoms, and there is a corresponding monotonic decrease in the activation energy.

4.4. IRC potential energy curve, $V(s)$ vs s

The potential energy curve, $V(s)$ vs s , for CF₂H₂...O is given in the Fig. 2, where the energy, E(UMP2), is plotted against the intrinsic reaction coordinate (IRC), s . All structures were optimized at the UMP2/6-311G** level. From this curve, the transmission coefficient κ was calculated, as discussed in Section 3.2. Similar curves were computed for the other reactants, and the corresponding κ values are presented in Table 6.

5. Discussion

Several correlations can be made from the data in Table 6, which show the dependence of the transmission coefficient, κ , imaginary normal-mode frequencies, ν , ΔG^\ddagger , and several TS distances upon the number of F-atom substitutions:

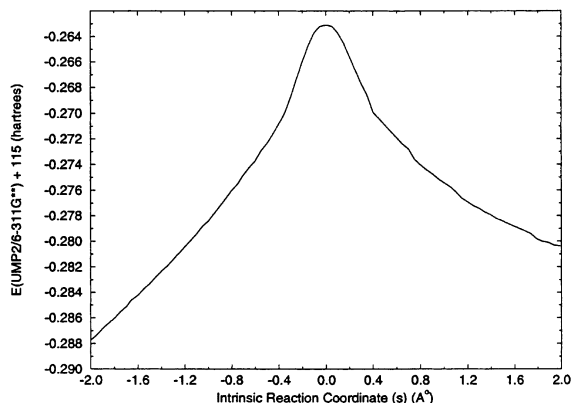


Fig. 2. Plot of the potential energy curve for the CH₄ TS, namely $V(s)$ versus s , where s is the intrinsic reaction coordinate (IRC). The values of $V(s)$ are the energies, E(UMP2), computed at the UMP2/6-311G** level with the IRC program. The origin of s corresponds to the TS, –115.26311 hartrees. From this curve, the transmission coefficient κ is calculated.

(i) The average difference between the theoretical and experimental values of ΔG^\ddagger for the four reactants is 1.3 ± 0.6 kcal/mol.

(ii) The variations of the C–H₂ and H₂–O distances with the number of F-atom substitutions show no discernable trend. However, the C–O distance is virtually constant, indicating a long-range interaction between the C and O atoms which is independent of the number of F atoms.

(iii) Ref. [15] shows that for a three-atom linear system the imaginary frequency is proportional to

Table 6

Dependence of the following quantities upon the number of F-atom substitutions in the TS: transmission coefficient κ , the imaginary normal-mode frequency ν , $\Delta G_{\text{theor.}}^{\ddagger}$ (kcal/mole), $\Delta G_{\text{expt'l}}^{\ddagger}$, the C–F (Å) distance, and several distances in the segment C–H₂–O^a

TS	κ	ν (cm ⁻¹)	$\Delta G_{\text{expt'l}}^{\ddagger}$	$\Delta G_{\text{theor.}}^{\ddagger}$	C–H ₂	H ₂ –O	C–O	C–F
CH ₄ ...O	1.14	2209i	14.67	14.00	1.284	1.182	2.466	–
CFH ₃ ...O	1.13	2368i	15.62	14.13	1.261	1.212	2.473	1.353
CF ₂ H ₂ ...O	1.10	2547i	15.34	14.71	1.264	1.206	2.470	1.334
CF ₃ H...O ^b	1.13	2645i	17.3	15.0	1.293	1.167	2.460	1.320

^aThe structures are all optimized at the UMP2/6-311G** levels, and the $\Delta G_{\text{theor.}}^{\ddagger}$ energies are at the \hat{G}_2 levels.

^bThese data are from Ref. [5]. The larger difference between $\Delta G_{\text{expt'l}}^{\ddagger}$ and $\Delta G_{\text{theor.}}^{\ddagger}$ is attributed to possible experimental uncertainty (only 1 datum in the region of 298 K), and/or a possible need for a higher computational level due to the large number of electrons.

the square root of the second derivative of the potential curve at the TS. We have estimated the approximate average second derivatives, $\bar{\Delta}^2$, near the top of the IRC curves (within ± 0.2 Å). We have obtained the following results: For CH₄...O, $\nu = 2209$ i cm⁻¹ and $\bar{\Delta}^2 = 0.00033$. For CF₂H₂, $\nu = 2547$ i cm⁻¹ and $\bar{\Delta}^2 = 0.00041$. The ratio of the ν 's is 1.15 and the ratio of the square root of the second derivatives is 1.11: these two quantities are approximately equal, as predicted in [15].

(iv) The values of $\Delta G_{\text{theor.}}^{\ddagger}$ increase with the number of F-atom substitutions. Also, there is an inverse correlation between the C–F distance and $\Delta G_{\text{theor.}}^{\ddagger}$, although surprisingly, there is no correlation between $\Delta G_{\text{theor.}}^{\ddagger}$ and the C–H₂ distance which is the actual breaking bond.

Table 5 presents the experimental C–H bond dissociation enthalpies (BDE's) for the homolytic dissociations $\text{CF}_n\text{H}_n \rightarrow \text{CF}_n\text{H}_{n-1} + \text{H}\cdot$, and the corresponding theoretical reaction enthalpies for the hydrogen abstraction by O(³P), ΔH_r . There is a correlation between the abstraction process, which involves a breaking of the C–H bond, and the BDE energies. This is seen in Table 5, where both the BDE and ΔH_r energies begin with high values, reach minima at the CFH₃ reactant, and end with high values. However, it should be pointed out that the $\Delta G_{\text{theor.}}^{\ddagger}$ energies in the hydrogen abstraction by O(³P) do not parallel the BDE energies, since the BDE energies reach a minimum at the CFH₃ reactant, whereas the $\Delta G_{\text{theor.}}^{\ddagger}$ energies are monotonic with the number of fluorine substitutions.

In reference to the large factor differences between the values of $k_{\text{expt'l}}$ and $k_{\text{theor.}}$, in Tables 2–4, we attribute these differences, in part, to uncertainties in the reported experimental values of

$B(E_a)$, n and A . For example, consider the case of the reactant CH₄. The 'recommended values' in [19] are used in Table 4. Now, let us use the values of $E_a = 9.00$ kcal/mol, $n = 0$ and $A = 3.5 \times 10^{13}$ from [26], which are valid at 298 K. These values yield $k_{\text{expt'l}} = 8.8 \times 10^6$ as compared with the value from Table 4, which is $k_{\text{expt'l}} = 3.0 \times 10^6$. Thus, the spread in reported experimental values results in a factor of about 3 between the $k_{\text{expt'l}}$ values. For the other two reactants, CFH₃ and CF₂H₂, there are only two experimental data and one experimental datum, respectively, and there are no recommended values.

In regard to our values of κ , several points should be pointed out:

(i) The authors in [9] report a large transmission effect which is larger than our value of κ due to the fact that they have taken into account small and large corner cutting curvature types of tunneling corrections (see [16] for details of such tunneling corrections, as well as the original paper by Marcus and Coltrin [27] for the H + H₂ reactions).

(ii) We have not considered such tunneling corrections because of the large increase in computational time that would be required for the four systems. Also, there would be the need to introduce the approximation that the exact system must be represented by a three-body approximation. Finally, we have obtained good agreement between our values of $\Delta G_{\text{expt'l}}^{\ddagger}$ and $\Delta G_{\text{theor.}}^{\ddagger}$ without using the corner cutting tunneling corrections.

(iii) In the three-body approximation, $\cdot\text{H} + \text{O} + \cdot\text{CH}_3$, the $\cdot\text{CH}_3$ grouping is considered rigid and enters in only via its mass. However, we have shown in our IRC computations that this grouping is not rigid if the whole system is optimized, because the angle aH_5CH_2 varies from

108.95° to 104.40° as the O atom approaches CH₄ (see Fig. 1 for a definition of this angle, in which figure two H's replace the two F's).

(iv) Finally, in Table 8 of [9], the ab initio rate constant, calculated with the ICVT mode, is in very good agreement with the experimental value of the rate constant at 300 K without the implementation of corner cutting tunneling corrections.

In reference to the HLC terms, we have observed that the HLC's for the activation-energy calculations cancel. For example, for the reactant, CH₄, the HLC's for the molecules, CH₄, O(³P) and CH₄...O are -0.030700, -0.018800 and -0.049500, respectively. The difference between the TS HLC and the reactant-sum HLC is 0.000.

6. Conclusions

The present results show that as the number of fluorine substitutions on the methane skeleton increases, the activation energy of the hydrogen abstraction by O(³P) increases. Also, the rate constants for this reaction decrease along this series. Tunneling, as calculated by the IRC program, increases the rate constants by 10–15% in the hydrogen abstractions by O(³P) at 298.15 K.

Comparisons with experimental data show that the $\hat{G}2$ theory yields accurate results for both structural features and thermodynamic activation properties for the fluorinated methanes, especially in the computations of the TS energies. These results will encourage the employment of this method for studies of other related systems, especially in systems for which experimental investigations have not been performed.

Acknowledgements

This study was supported in part by NSF/PSC Grant No. CHE890046P and PSC/NPACI/SDSC Grant No. WRI200. W.C.K. wishes to thank the director and the staff of CaTS at Wright State University for their continued support.

References

- [1] W.E. Wilson, J.T. O'Donovan, *J. Chem. Phys.* 48 (1968) 2829.
- [2] D. Henschler, in: M.W. Anders (Ed.), *Bioactivation of Foreign Compounds*, Academic Press, New York, 1988, pp. 317–346.
- [3] M.W. Anders, L.R. Pohl, *Bioactivation of Foreign Compounds*, Academic Press, New York, 1988, pp. 283–315.
- [4] M.L. Gargas, P.G. Seybold, M.E. Andersen, *Toxicol. Lett.* 43 (1988) 235.
- [5] W.C. Kreye, *Chem. Phys. Lett.* 256 (1996) 383.
- [6] A. Bottoni, G. Poggli, S.S. Emmi, *J. Molec. Struct. (Theochem.)* 279 (1993) 299.
- [7] J.L. Durant Jr., C.M. Rohlging, *J. Chem. Phys.* 98 (1993) 8031.
- [8] O. Roberto-Neto, F.B.C. Machado, D.G. Truhlar, *J. Chem. Phys.* 111 (1999) 10046.
- [9] M. González, J. Hernando, J. Millán, R. Sayós, *J. Chem. Phys.* 110 (1990) 7326.
- [10] T. Yamada, T.D. Fang, P.H. Taylor, R.J. Berry, *J. Phys. Chem.* 104 (2000) 5013.
- [11] C. Gonzalez, J.J.W. McDouall, H.B. Schlegel, *J. Phys. Chem.* 94 (1990) 7467.
- [12] M.J. Frisch et al., *GAUSSIAN 98*, Gaussian, Pittsburgh, PA, 1998.
- [13] L.A. Curtiss, K. Raghavachari, G.W. Trucks, J.A. Pople, *J. Chem. Phys.* 94 (1991) 7221.
- [14] C. Gonzalez, H.B. Schlegel, *J. Chem. Phys.* 90 (1989) 2154.
- [15] S. Glasston, K.J. Laidler, H. Eyring, *The Theory of Rate Processes*, McGraw-Hill, New York, 1941, pp. 116–121, 198.
- [16] D.G. Truhlar, A.D. Isaacson, B.C. Garrett, in: M. Bauer, (Ed.), *Theory of Chemical Reaction Dynamics*, CRC Press, Boca Raton, FL, 1985, pp. 66–137.
- [17] B.C. Garrett, D.G. Truhlar, *J. Phys. Chem.* 83 (1979) 2921.
- [18] M.W. Chase, C.A. Davies, J.R. Downey Jr., D.J. Fruurip, R.A. McDonald, A.N. Syverud, *J. Phys. Chem., Ref. Data*, 14, 1985; Supplement No. JANAF Thermochemical Tables, third ed., Part I. Al-CO.
- [19] J.T. Herron, *J. Phys. Chem., Chemical Kinetic Ref. Data* 17 (1988) 967.
- [20] A.E. Reed, R.B. Weinstock, F. Weinhold, *J. Chem. Phys.* 83 (1985) 735.
- [21] K.C. Gross, P.G. Seybold, *Int. J. Quantum Chem.* 80 (2000) 1107.
- [22] M.H. Bhagal-Vayjooee, A.J. Colussi, S.W. Benson, *Int. J. Chem. Kinet.* 11 (1979) 147.
- [23] J.M. Pritchard, A.S. Rodgers, *Int. J. Chem. Kinet.* 15 (1983) 569.
- [24] J. Heicklin, *Int. J. Chem. Kinet.* 13 (1981) 651.
- [25] D.C. McKean, J.L. Duncan, L. Batt, *Spectrochim. Acta* 29A (1973) 1037.
- [26] J. Barassin, J. Combourieu, *Bull. Chem. Soc. France* 1 (1974).
- [27] R.A. Marcus, M.E. Coltrin, *J. Chem. Phys.* 67 (1977) 2609.